Available online at www.sciencedirect.com
ScienceDirect
European Journal of Medicinal Chemistry 43 (2008) 2877–2890
EUROPEAN JOURNAL OF MEDICINAL CHEMISTRY
http://www.elsevier.com/locate/ejmech

Short communication

Synthesis, antitumor evaluation and DNA binding studies of novel amidino-benzimidazolyl substituted derivatives of furyl-phenyl- and thienyl-phenyl-acrylates, naphthofurans and naphthothiophenes

Marijana Hranjec [a], Kristina Starčević [a], Ivo Piantanida [b], Marijeta Kralj [c], Marko Marjanović [c], Merima Hasani [d], Gunnar Westman [d], Grace Karminski-Zamola [a,*]

[a] *Department of Organic Chemistry, Faculty of Chemical Engineering and Technology, University of Zagreb, Marulićev trg 20, P.O. Box 177, HR-10000 Zagreb, Croatia*
[b] *Division of Organic Chemistry and Biochemistry, Laboratory of Supramolecular and Nucleoside Chemistry, Ruđer Bošković Institute, Bijenička cesta 54, P.O. Box 180, HR-10000 Zagreb, Croatia*
[c] *Division of Molecular Medicine, Laboratory of Functional Genomics, Ruđer Bošković, Institute, Bijenička cesta 54, P.O. Box 180, HR-10000 Zagreb, Croatia*
[d] *Department of Chemistry and Bioscience, Chalmers University of Technology, S-412 96 Göteborg, Sweden*

Received 11 October 2007; received in revised form 30 January 2008; accepted 8 February 2008
Available online 29 February 2008

Abstract

A series of amidino-substituted benzimidazoles, related to furyl-phenyl- and thienyl-phenyl-acrylates, naphthofurans and naphthothiophenes were prepared, their antitumor evaluation and interactions with ct-DNA have been investigated. All tested compounds show differential and strong antitumor activity without apparent difference depending on their structures. Interestingly, the MCF-7 tumor cell line is highly sensitive to all compounds. Compounds **6**–**9** showed noticeable selectivity in regard to normal fibroblasts (WI 38). Compounds **4**–**9** interact with ct-DNA by more binding modes, whose mutual distribution is dependent on the compound/DNA ratio. The ''acyclic'' **4**–**6** and ''cyclic'' compound **7** interact mostly within the minor groove of DNA, although partial intercalation of **6** and **7** cannot be excluded. The ''cyclic'' compounds **8** and **9** intercalate between DNA base pairs at high excess of DNA over compounds.
© 2008 Elsevier Masson SAS. All rights reserved.

Keywords: Benzimidazoles; Amidines; Photocyclization; Antitumor evaluation; DNA binding

1. Introduction

DNA plays a major role in the life process because it carries heritage information and instructs the biological synthesis of proteins and enzyme through the process of replication and transcription of genetic information. An understanding of the drug–DNA interactions is a promising approach to developing novel reagents and plays a key role in pharmacology today [1,2]. Due to interaction of many biologically active compounds with biomolecules, they represent a major target in drug development strategies designed to produce next generation therapeutics for diseases such as cancer [3,4].

Over the past years there is a considerable interest in the development and pharmacology of heteroaromatic organic compounds, such as benzimidazoles [5,6], due to their wide range of biological activity as antitumor [7,8,9], antibacterial [10,11], antifungal [12] or antiviral [13,14] agents. Benzimidazole substituted derivatives are also inhibitors of cyclin-dependent kinase or tyrosine kinase and are useful for inhibiting cell proliferation for the treatment of cancer [15,16,17]. The fact that benzimidazole residue is a constituent of vitamin B12 supports their potential use as therapeutics. Due to the structural similarity of benzimidazole nuclei with some naturally occurring compounds such as purine, they can easily

* Corresponding author. Tel.: +385 14597215; fax: +385 14597250.
E-mail address: gzamola@pierre.fkit.hr (G. Karminski-Zamola).

0223-5234/$ - see front matter © 2008 Elsevier Masson SAS. All rights reserved.
doi:10.1016/j.ejmech.2008.02.010

interact with biomolecules of the living systems. Bis(benzimidazole) derivatives as Hoechst 33342 and 33258 (Fig. 1) also bind in the minor groove of DNA [18,19]. Hoechst 33258 has undergone Phase I clinical evaluation as an anticancer agent and the inhibition of topoisomerase and DNA helicase has been proposed as its mechanism of action [20,21].

On the other hand, amidines are structural parts of numerous compounds of biological interest including important medical and biochemical agents [22,23]. Some aromatic diamidines such as pentamidine, berenil or furamidine (Fig. 2) are minor groove binding agents and are used in the treatment of several protozoan diseases based on their selective binding to AT rich sequences of DNA helix [24].

Recently we reported about the synthesis and antitumor evaluation of some new amidino benzimidazolyl substituted naphtho[2,1-*b*]furan carboxylates [25] as well as synthesis, antitumor evaluation and DNA binding of heteroaromatic acyclic and cyclic amidino-substituted naphthofuran or naphthothiophene carboxylates [26]. As a part of our continuing search for potential anticancer agents, herein we present the synthesis of acyclic and cyclic condensed heterocyclic benzimidazole derivatives, related to naphthofurans and naphthothiophenes (Fig. 3), as well as their antitumor evaluation on several human tumor cell lines and detailed DNA binding studies of all synthesized compounds.

2. Results and discussion

2.1. Chemistry

All compounds **4**–**9** shown in Fig. 3 were prepared according to Scheme 1. Acyclic amidino-substituted compounds **4**–**6** were prepared by condensation of corresponding heterocyclic aldehydes **1**–**3** and 4-isopropylamidino-1,2-phenylendiamine [27] in the yields of about 30–51% [25]. We prepared only isopropyl-amidines because our earlier obtained results showed that isopropylamidino-substituted compounds have shown in most cases more pronounced biological activity [25,26a]. Aldehydes **1**–**3** were prepared by earlier described methods [26]. In the reaction of photochemical dehydrocyclization [28], acyclic compounds **4**–**6** were converted into their cyclic products **7**–**9** in the yields of about 35–59%.

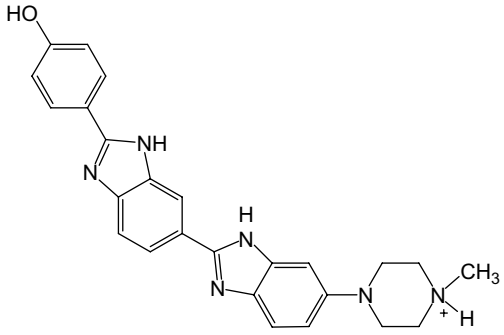

Hoechst 33258

Fig. 1. Chemical structure of Hoechst 33258.

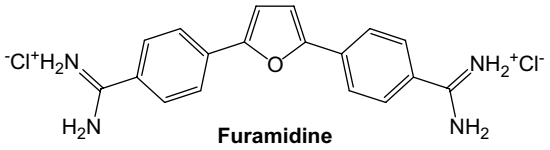

Furamidine

Fig. 2. Chemical structure of furamidine.

Synthesis of compounds **4** and **7** has already been published [25].

Furyl-phenyl-acrylates can be viewed as a heterocyclic analogue of substituted stilbene [29]. Heterocyclic acrylates are photochemically active [30,31] and the expected photoreactions, by analogy with stilbenes and related compounds [32], are *E*/*Z* photoisomerization from excited singlet state and ring-closure reaction from the *E* isomers to form reversibly the dihydro *trans*-adduct intermediate by electrocyclic reaction. Under oxidative conditions the dihydro intermediate is converted to the desired naphtho[2,1-*b*]furan-5-carboxylate.

In our previous paper [33] we described experiments that present the conceptual basis for the development of new photoinduced anticancer therapy based on the photochemical transformation of a DNA/RNA inactive into an active one. Additional advantage of this concept is to access a large number of already known or new molecules with selected properties compatible with physiologically relevant conditions. In order to obtain new systems capable to undergo the photoinduced dehydrocyclization by visible light irradiation, we prepared previously described benzimidazole derivatives of *E*-methyl-3-(2-furyl)-2-phenyl-acrylate.

2.2. Interactions of compounds *4*–*9* with ct-DNA

2.2.1. Spectroscopic properties of compounds *4*–*9*

Compounds studied in this paper are divided in two groups, ‘‘acyclic’’ derivatives (Fig. 3; **4**–**6**) and their ‘‘cyclic’’ photoproducts (Fig. 3; **7**–**9**). Since for DNA binding studies of above-mentioned compounds application of spectrophotometric methods was necessary, we have characterized aqueous solutions of all compounds by means of electronic absorption (Fig. 4, Table 1) and fluorescence emission spectra (Fig. 5).

Absorbencies of aqueous solutions of compounds are proportional to their concentrations up to 2.08×10^{-5} mol dm^{-3} (**4**), 1.67×10^{-5} mol dm^{-3} (**5**), 2.82×10^{-5} mol dm^{-3} (**6**), 1.26×10^{-5} mol dm^{-3} (**7**), 5.45×10^{-5} mol dm^{-3} (**8**), and 2.11×10^{-5} mol dm^{-3} (**9**), indicating that there is no significant intermolecular stacking which should give rise to hypochromic effect. Aqueous solutions of all studied compounds were shown to be stable over longer period.

Comparison of UV–vis spectra of both, ‘‘acyclic’’ (**4**–**5**) and ‘‘cyclic’’ (**7**–**8**) furan derivatives, pointed out that introduction of electron-withdrawing group (–CN) on the phenyl ring resulted in bathochromic shift of absorption maxima, as well as hypochromic effect. The thiophene derivatives (**6** and **9**) are characterized by significantly lower molar absorptivities (ε) and absorption maxima shifted toward longer wavelengths in comparison to furan analogues (**4** and **7**).

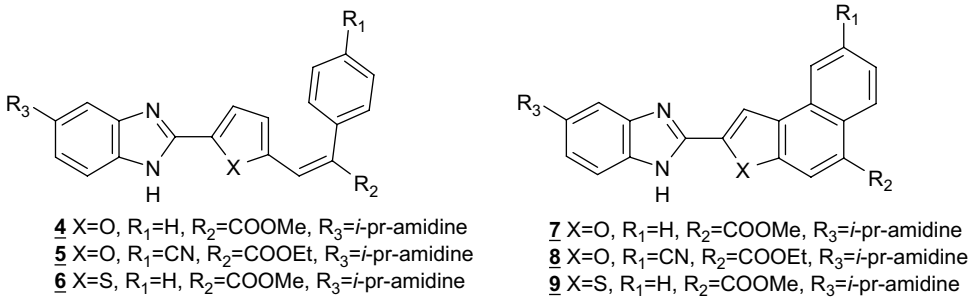

Fig. 3. Amidino-substituted "acyclic" **4–6** and "cyclic" **7–9** benzimidazole derivatives.

All studied compounds exhibit characteristic fluorescence emission with maxima at 419–428 nm (Table 2). Their excitation spectra are in good agreement with absorption spectra.

Comparison of fluorescence spectra (Table 2, Fig. 5) revealed that emission of "acyclic" compounds **4–6** is significantly weaker if compared to their "cyclic" analogues **7–9**, most likely due to the more efficient conjugation of rigid, planar, cyclic moieties, while ethene linker of "acyclic" compounds is characterized by significantly higher motional freedom and thus upon excitation allows more modes of non-emissive relaxation. It should be stressed that fluorescence emission of "acyclic" compounds **4–6** is stable under experimental conditions used, pointing out that photoinduced cyclisation into "cyclic" analogues **7–9** does not take place; otherways due to the significantly stronger fluorescence of "cyclic" analogues compared to "acyclic", permanent irradiation in the fluorimeter should result in substantial emission increase. It is interesting to note that furan derivatives **4** and **7** exhibit more than at least order of magnitude stronger fluorescence compared to their thiophene derivatives **6** and **9**. Intriguingly, introduction of cyano group on benzene moiety strongly decreased the fluorescence of furan derivatives **5** and **8** when compared to unsubstituted analogues **4** and **6**. That could be correlated to the strong electron-withdrawing properties of cyano group and points out the pronounced impact of the electronic properties of here presented molecules on the ratio between non-emissive and emissive relaxation.

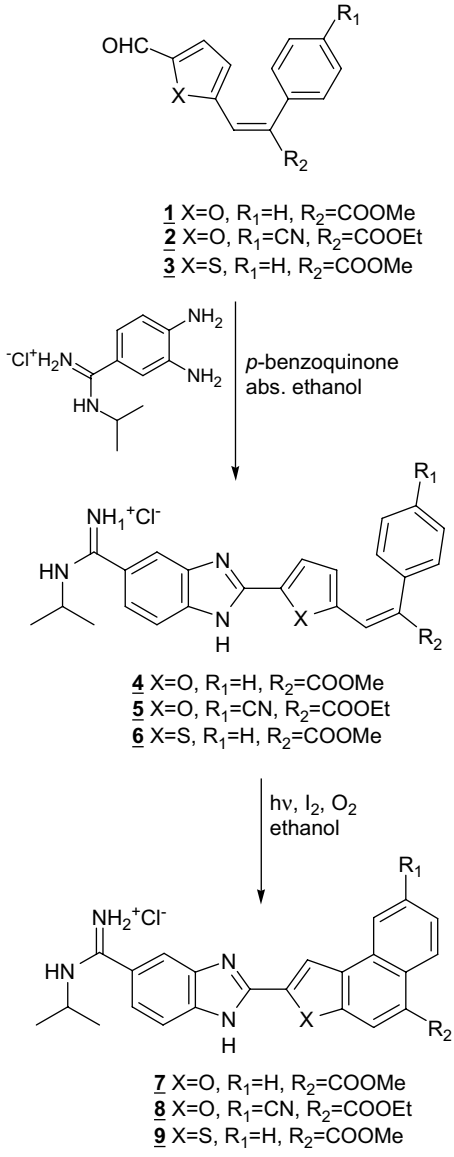

Scheme 1. Synthesis of amidino-substituted benzimidazole derivatives.

2.2.2. UV–vis titrations with ct-DNA

The UV–vis spectra of all studied compounds exhibited strong hypochromic and bathochromic changes upon addition

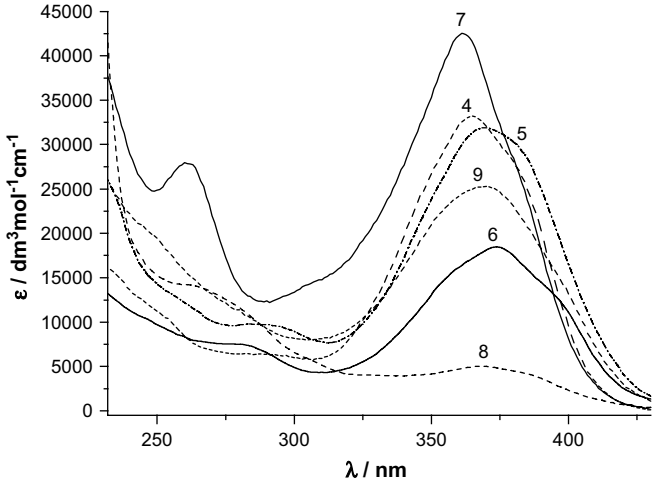

Fig. 4. UV–vis spectra of studied compounds.

Table 1
Electronic absorption maxima and corresponding molar extinction coefficients of studied compounds in water

Compound	λ_{max}/nm	$\varepsilon \times 10^3$ dm^3 mol^{-1} cm^{-1}
4	366	33.6
5	370	31.7
6	374	18.4
7	362	42.2
	260	28.8
8	367	5.0
	263	14.2
9	370	24.5
	225	27.1

of ct-DNA at conditions of excess of compound over DNA base pairs (ratio $r > 0.5$) (Table 3).

However, further additions of ct-DNA leading to excess of DNA base pairs over compound ($r < 0.5$) resulted in hyperchromic effect and additional bathochromic shift of maxima in the UV–vis spectra of all studied compounds except **5**. Therefore, only for compound **5** it was possible to process titration data by means of Scatchard equation to obtain binding constant $\log Ks = 5.6$ and ratio $n_{[\mathbf{5}]/[\text{ct-DNA}]} = 0.5$. All compounds, whose UV–vis spectra exhibit changes in opposite directions depending on the compound/ct-DNA ratio, obviously form at least two different types of complexes with ct-DNA. Interestingly, at excess of ct-DNA over compound peculiar UV–vis maximum splitting can be observed exclusively for "cyclic" furan derivatives **7** and **8**, but not for "acyclic" analogues **4**–**6** as well as "cyclic" thiophene derivative **9** (Fig. 6).

Rather small changes in UV–vis spectra as well as the presence of at least two different types of complexes with ct-DNA didn't allow calculation of binding constants ($\log Ks$) for most of the compounds.

2.2.3. Fluorimetric titrations with ct-DNA

Addition of ct-DNA yielded strong increase of fluorescence emission of "acyclic" derivatives, almost linearly dependent to the c(ct-DNA) even at extremely high excess of base pairs

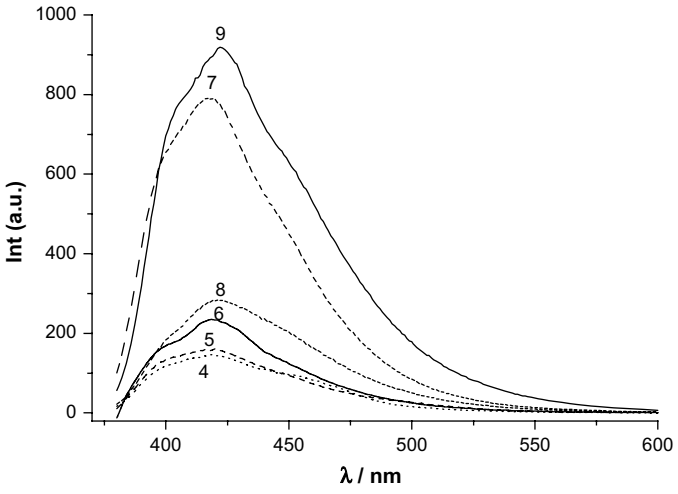

Fig. 5. Fluorescence emission spectra of studied compounds, c(**4**, **7**) $= 2.4 \times 10^{-8}$ mol dm^{-3}, c(**5**, **6**, **8**, **9**) $= 3.6$–3.9×10^{-7} mol dm^{-3}.

Table 2
Fluorescence emission and excitation properties of studied compounds in water

Compound	c_s/mol dm^{-3}	λ_{emiss}/nm	λ_{exc}/nm	Rel. fluo. int. (a.u.)	$\text{Int}_{\text{cyclic}}/\text{Int}_{\text{acyclic}}$
4	2.4×10^{-8}	425	365	147.1	–
7	2.4×10^{-8}	419	360	790.1	5.37
5	3.6×10^{-7}	425	370	161.4	–
8	3.7×10^{-7}	426	368	282.2	1.75
6	3.8×10^{-7}	428	374	231.8	–
9	3.9×10^{-7}	424	370	916.1	3.95

over compounds (Fig. 7). Such a linear dependence is not in accord with the UV–vis titrations, which pointed toward the end of titration at much lower ct-DNA concentrations. Such a discrepancy could be the result of other processes monitored by fluorescence simultaneously proceeding with titration. Therefore it was not possible to process titration data by means of Scatchard equation in order to obtain binding affinity (Table 4).

Similarly as observed in the UV–vis titration experiments, titration with ct-DNA resulted in opposite changes of fluorescence of "closed" analogues **7**–**9** depending on the compound/ct-DNA ratio r. Namely, at excess of DNA strong fluorescence quenching was observed, while ratios $r < 0.2$–0.5 yielded strong increase of **7**–**9** fluorescence. Excellent fitting of the titration data at high excess of ct-DNA over compounds ($r \ll 0.1$) to Scatchard equation pointed to the existence of only one dominant type of complex and allowed calculation of binding constants ($\log Ks$, Table 4). The obtained results (Table 4) point toward similar affinity of all "cyclic" compounds toward ct-DNA, which is also comparable to previously studied analogues [26,33].

2.2.4. Thermal melting experiments

Interactions of compounds **4**–**9** with ct-DNA were also studied by thermal melting experiments according to Table 5.

The "acyclic" furan derivative **4** does not cause any thermal stabilization of ct-DNA, while its "cyclic" analogue **7** stabilized DNA double helix. However, this is not the case for **5**, **6**, **8** and **9**, since "acyclic" analogues **5** and **6** also thermally stabilize ct-DNA. That observation could be correlated to differences in the electronic absorption and fluorescence spectra of **4** and **7** when compared to **5**, **6**, **8** and **9**. That points toward significant impact of electron-withdrawing group (–CN) as well as exchange of furan with thiophene on the electronic properties of compounds and consequently influences their interactions with ct-DNA.

2.2.5. Flow linear dichroism

Linear dichroism (LD) is the difference in absorption of polarized light perpendicular and parallel to an orientation axis. Since the electronic transitions of the DNA bases are perpendicular to the DNA helix axis they will give rise to a negative LD. Thus, intercalating ligands will also have a negative LD whereas minor groove binding compounds have a positive signal.

Table 3
Changes of UV–vis spectra upon titration with ct-DNA

	4[c]	**7**[c]	**5**	**8**[c]	**6**[c]	**9**[c]
H[b]/%	8% decrease up to $r = 0.7$, then increases	51% decrease up to $r = 1$, then increases	10% decrease	10% decrease up to $r = 2$, then increases	18% decrease up to $r = 0.38$, then increases	15% decrease up to $r = 0.5$, then increases
$\Delta\lambda$[a]	+7 nm	+8 and +15 maximum splitting	+7 nm	+7 and +11 maximum splitting	+8 nm	+8 nm
log *K*s/*n*	–	–	5.6/0.5$_{fix}$	–	–	–

[a] Shift of the absorbance maximum; $\Delta\lambda = \lambda$ (complex) $- \lambda$ (compound); absorbance maxima λ_1 (**4**: $\lambda = 366$ nm, **7**: $\lambda = 362$ nm, **5**: $\lambda = 370$ nm, **8**: $\lambda = 367$ nm, **6**: $\lambda = 374$ nm, **9**: $\lambda = 370$ nm).
[b] Hypochromic effect. $H = (\text{Abs(compound)} - \text{Abs(complex)})/\text{Abs(compound)} \times 100$.
[c] Changes in opposite direction – first decrease, then increases.

Flow linear dichroism (LD) was used to determine the orientation of the molecules bound to DNA. Flow LD spectra were measured for the dyes in presence of calf thymus DNA (ct-DNA) at two different mixing ratio, namely, dye/base pair, of 1:24 and 1:4 (Fig. 8).

From the LD measurements it was found that the acyclic derivatives **4** and **5** showed a positive LD signal indicating minor groove binding. Compound **6** showed only a weak LD signal. All three of them showed a higher LD signal at the higher ratio, 1:24 dye/base pair, of DNA. At the ratio 1:4 dye/base pair they showed a weaker LD signal indicating that the dyes are bound in a more randomized way when they are tightly packed in the DNA. The cyclic derivatives **8** and **9** showed almost no LD signal which indicates that the molecules are bound in a random way at this mixing ratio. If the cyclic derivatives **8** and **9** would only bind intercalatively the LD spectra should show a negative LD signal. Since this is not the case one can assume that the dye binds in a randomized way. Interestingly, the cyclic derivative **7** showed LD signal, suggesting that it binds in the groove of DNA.

2.2.6. Circular dichroism

Upon binding of achiral molecules to chiral environments such as the grooves of DNA achiral compounds show CD signal which is characteristic of their interaction with DNA. Compared to the intercalation site between the base pairs, the minor groove of DNA provides a more chiral environment affording a larger ICD of minor groove binders.

Compounds **4**, **5**, and **7** that showed the highest LD signals are also the compounds that show the highest ICD signal, verifying groove binding (Fig. 9).

2.2.7. Discussion of results

In the UV–vis titrations all studied compounds except **5** showed mixed binding modes toward ct-DNA, with spectroscopic breakpoints at about $r = 0.2$–2. However, there is distinct difference between ''acyclic'' and ''cyclic'' analogues, UV–vis spectra of latter showing much more pronounced bathochromic and hypochromic effect upon addition with ct-DNA.

The ''acyclic'' analogues **4**–**6** yield low or no thermal stabilization of ct-DNA. The affinity toward DNA was estimated only for **5** from the UV–vis titration data (log *K*s = 5.6, $n = 0.5$ – ratio too high for intercalation but agreeable to minor groove binding), while for **4** and **6** it was not possible to estimate due to the mixed binding modes obvious in the UV–vis titrations and inconsistency of emission changes in fluorimetric titrations. All ''acyclic'' analogues show positive LD signal providing strong indication of DNA minor groove binding. However, there is distinctive difference in CD experiments between **4**, **5** on one side and **6** on other side. Namely, **4** and **5** showed strong positive ICD signal also supporting minor groove binding, while **6** showed ICD signal which is negative – positive couplet – the origin of this is not clear yet but it could be correlated to the fact that among the ''acyclic'' analogues **6** yielded by far highest thermal stabilization of ct-DNA.

The ''cyclic'' analogues **7**–**9** yielded considerable thermal stabilization of ct-DNA. The UV–vis and fluorimetric titrations revealed that all ''cyclic'' compounds form at least two different types of complexes with ct-DNA. Fortunately, in fluorimetric titrations it was possible to collect enough data at conditions of high excess of DNA over compounds. At such conditions one type of complex was dominant, which allowed calculation of binding constants by Scatchard equation (log *K*s, Table 4). Obtained log *K*s values were similar for all studied compounds as well as comparable to previously studied analogues [26,33]. The ''cyclic'' analogues **8** and **9** showed very weak LD signal upon addition of ct-DNA indicating a mixture of binding modes, which agreed nicely with results of UV–vis and fluorescence titrations collected close to equimolar compound/DNA ratios. The CD experiments revealed quite different effect induced by each of ''cyclic'' analogues. The addition of ct-DNA to **8** yielded almost no ICD signal at $\lambda > 300$ nm. Compound **7** showed positive ICD signal, whose shape was dependent on the **7**/base pair ratio. Compound **9** showed weak, negative ICD signal only at high excess of ct-DNA, pointing toward intercalative binding mode. Since all other parameters of **7**–**9** interactions with ct-DNA were generally comparable (affinity toward ct-DNA, changes in fluorescence and UV–vis spectra, ΔT_m experiments), differences in CD experiments suggest that the cyclic compound **7** seems to have a clear preference for minor groove binding (positive LD and ICD signals) [35], which is not the case for the other two cyclic compounds (**8** and **9**). Possible reason for that may be that the oxygen in the cyclic ring formed

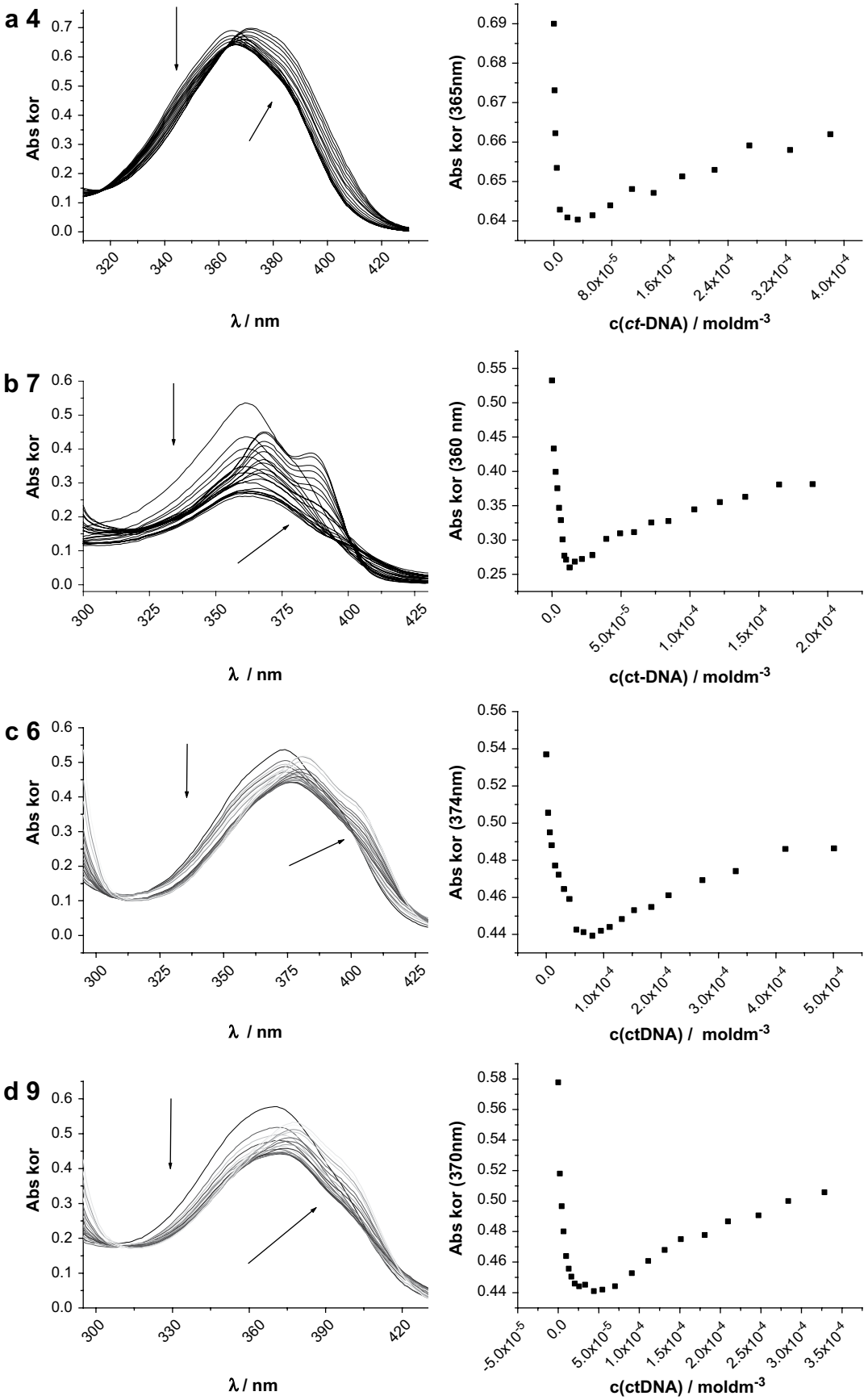

Fig. 6. UV–vis spectral changes of (a) **4** ($c = 2.04 \times 10^{-5}$ mol dm^{-3}), (b) **7** ($c = 1.26 \times 10^{-5}$ mol dm^{-3}), (c) **6** ($c = 2.96\ 10^{-5}$ mol dm^{-3}) and **9** ($c = 2.34 \times 10^{-5}$ mol dm^{-3}) upon the addition of ct-DNA ($c = 6.31 \times 10^{-3}$ mol dm^{-3}); sodium cacodylate/HCl buffer, $I = 0.05$ mol dm^{-3}, pH 7.

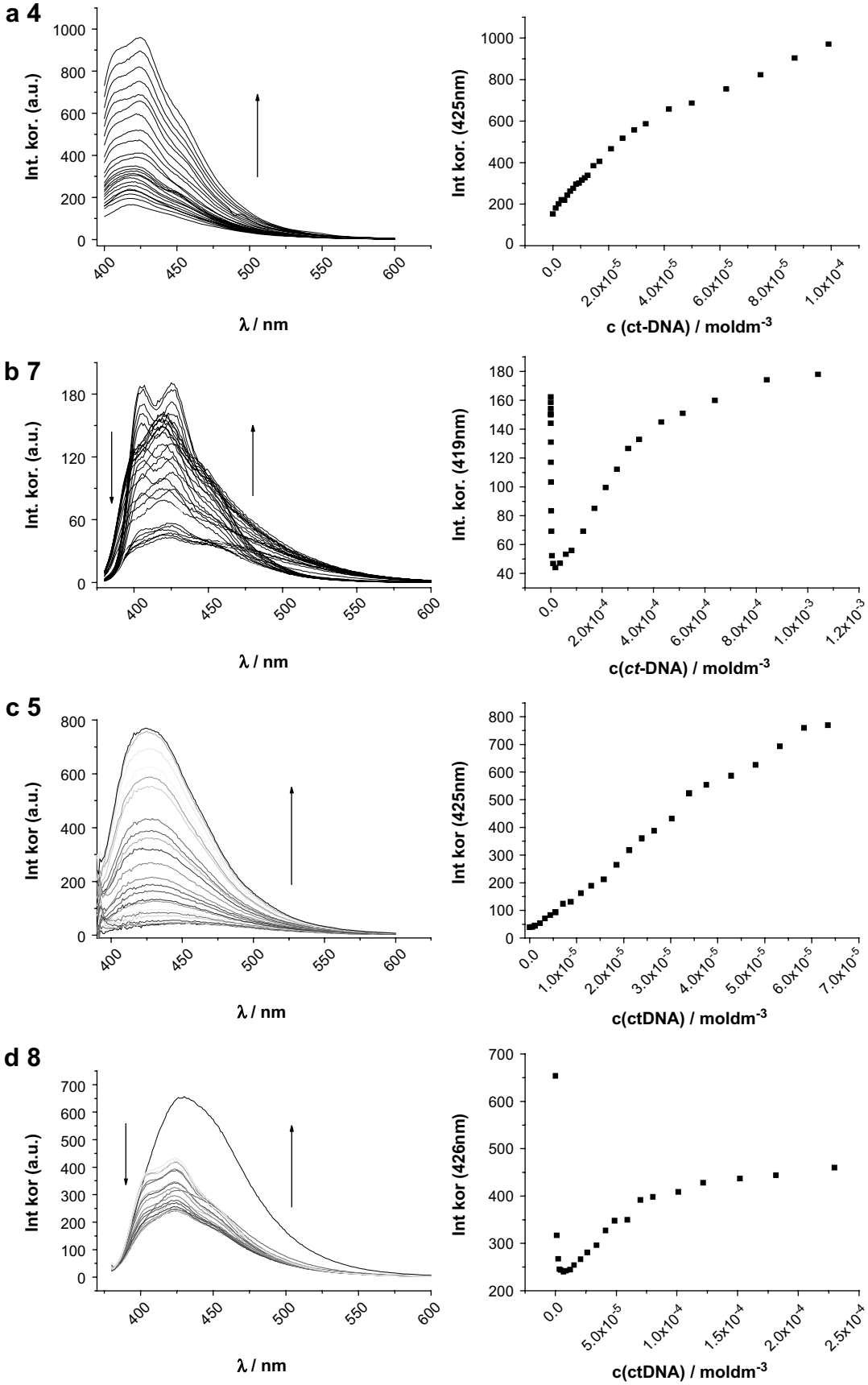

Fig. 7. Fluorescence emission of (a) **4** ($c = 3.7 \times 10^{-6}$ mol dm^{-3}), (b) **7** ($c = 5.3 \times 10^{-6}$ mol dm^{-3}), (c) **5** ($c = 3.4 \times 10^{-7}$ mol dm^{-3}) and (d) **8** ($c = 2.9 \times 10^{-6}$ mol dm^{-3}) upon the addition of ct-DNA ($c = 6.31 \times 10^{-3}$ mol dm^{-3}); sodium cacodylate/HCl buffer, $I = 0.05$ mol dm^{-3}, pH 7.

Table 4
Binding constants (log *K*s) calculated from the fluorimetric titrations[a] with ct-DNA at pH = 7.0 (buffer sodium cacodylate, $I = 0.05$ mol dm^{-3})

No.	**4**	**7**	**5**	**8**	**6**	**9**
log *K*s	–	4.2	–	5.0	–	4.7
n[a]	–	0.2	–	0.2	–	0.2
ΔInt[b]	Linear increase after $r = 0.1$	70% decrease up to $r = 0.16$ then increases about 6× with 0.1 M NaCl similar	Linear increase	60% decrease up to $r = 0.5$ then increases 50%	Linear increase after $r = 0.01$	61% decrease up to $r = 0.16$ then increases 9–13×

[a] Titration data at $r_{[\text{compound}]/[\text{ct-DNA}]} < 0.1$ were processed according to the Scatchard equation; the fixed value of ratio $n_{[\text{bound compound}]/[\text{ct-DNA}]} = 0.2$ was chosen for easier comparison with previously obtained log *K*s values [26,33].
[b] Change of fluorescence; ΔInt = Int(complex)/Int(compound).

hydrogen bonds with amino groups on DNA bases. Namely, our previous results [34] pointed out that two compounds with the only difference that one had a benzothiazole substituent and the other one had a benzoxale substituent exhibited different binding modes toward DNA. The oxygen derivative, BOXTO, interacted with DNA in a more homogeneous way whereas the sulphur analogue, BETO, exhibited more heterogenic interactions. Compound **9** according to the weak negative ICD signal [35] presumably binds dominantly by intercalation at high excess of ct-DNA, while single binding mode of compound **8** is not clearly defined, but most likely binds by intercalation at high excess of ct-DNA.

2.3. Biological results

All tested compounds showed evident antiproliferative effect on the presented panel cell lines (Table 6 and Fig. 10A–F), with IC_{50} ranging from 1–85 μM. Except **4**, which showed in general non-selective growth inhibition of all cell lines, all other compounds show very differential and strong antiproliferative activity without obvious difference depending on their structures. Compounds **6–9** showed noticeable selectivity in regard to normal human fibroblasts (WI 38), being clearly less cytotoxic to normal than to tumor cell lines. Most interesting, however, is the high sensitivity of MCF-7 tumor cell line to all compounds. We have already noticed this phenomenon in our previous work [13] in which 2-substituted-5-amidino-benzimidazoles were tested. The observed selectivity toward breast cancer cells should be correlated to benzimidazole moiety, since similar apparent selectivity of various benzimidazoles to breast cancer cells has also been previously shown by other authors [36,37]. Moreover, several compounds of benzimidazole class that have predominantly been utilized as antifungal and antihelminthic agents, such as Mebendazole [38] oncodazole and methyl-2-benzimidazolecarbamate (Carbendazim, FB642) have also been investigated as potential antitumor drugs. Interestingly, the antitumor activity of FB642 against MCF-7 breast tumor xenografts in mice was among the highest for all tumor models studied and was also better than either paclitaxel or vinorelbine. Although different modes of action of various benzimidazoles have been described in the literature (e.g. DNA groove binding, topoisomerase I or II inhibition, interactions with microtubules, inhibition of tumor helicases), selective growth inhibitory activity toward breast cancer cells could also be explained by selective induction of cytochrome P450 (CYP-1) enzymes especially in MCF-7 line, since it is known CYP-1 inducible cell line [39]. These enzymes catalyze the initial step in either detoxification or bioactivation of environmental toxins and xenobiotics [40]. The transcriptional regulation of the CYP1A1 gene by polycyclic aromatic hydrocarbons (PAH) and halogenated aromatic hydrocarbons (HAH) is mediated via ligand-dependent activation of the aryl hydrocarbon receptor (AhR), which translocates to the nucleus upon activation, dimerizes to the aryl hydrocarbon receptor nuclear translocator (arnt) protein and binds to the xenobiotic response element (XRE) in the regulatory region of the CYP1A1 gene [41]. Although benzimidazole compounds do not conform to the structural features of AhR ligands (planar hydrophobic aromatic compounds and aryl amines) and, accordingly, do not bind with high specificity to the AhR, it has been shown that several sulphur-containing benzimidazole drugs induce cytochrome P450 in humans and rodents. Among them are some of the above-mentioned anthelmintic drugs [42]. Therefore, the mechanism of induction of CYP1A by the benzimidazoles has been under debate and the results indicate that benzimidazoles activate the AhR complex by a novel intracellular mechanism distinct from those exerted by AhR ligands and which may have components in common with an endogenous activation mechanism for the AhR. It is possible that their degradation products constitute ligands of the AhR [42]. Similar concept has been shown concerning the discovery of a class of 2-(4-aminophenyl)benzothiazoles, candidate antitumor agents that showed remarkably similar highly selective profiles of antitumor activity. Although these compounds acted different from all known arylamines, a series of investigation proved that CYP1A1 and CYP1B1 activation leads to their toxicity through DNA [43].

Table 5
ΔT_m values[a] (°C) of ct-DNA upon addition of different ratios r[b] of **4–9** at pH = 7.0 (buffer sodium cacodylate, $I = 0.05$ mol dm^{-3})

r[b]	**4**	**7**	**5**	**8**	**6**	**9**
0.1	0	1.8	0.6	1.0	1.7	3.9
0.2	0	2.6	0.8	1.4	2.3	4.9
0.3	0	3.8	1.3	1.6	2.7	5.8

[a] Error in ΔT_m: ±0.5 °C.
[b] r = [compound]/[polynucleotide].

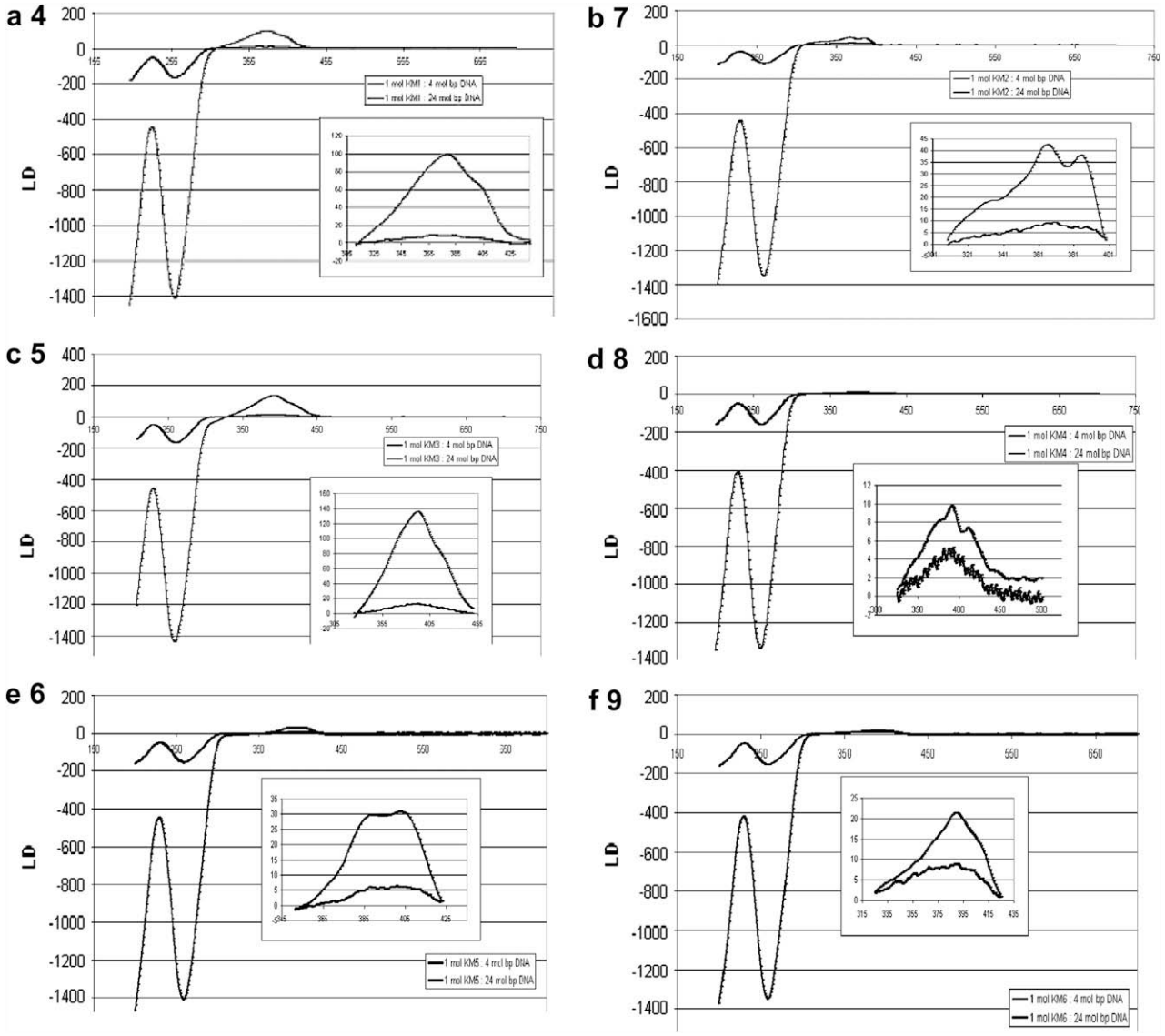

Fig. 8. Flow LD spectra of compounds **4**–**9** in the presence of ct-DNA at two different mixing ratios, namely, dye/base pair, of 1:24 and 1:4.

3. Conclusions

All tested compounds show very differential and strong antitumor activity without apparent difference depending on their structures. Compounds **6**–**9** showed noticeable selectivity in regard to normal human fibroblasts (WI 38). The most interesting observation is the high sensitivity of MCF-7 tumor cell line to all compounds. We can conclude that the observed selectivity toward breast cancer cells should be correlated to benzimidazole moiety, which selectively induce cytochrome P450 (CYP-1) enzymes especially in MCF-7 line, since it is known CYP-1 inducible cell line. These enzymes catalyze the initial step in either detoxification or bioactivation of environmental toxins and xenobiotics. Similar observations in MCF-7 cells treated with various benzimidazoles were also noticed previously.

All studied compounds interact with ct-DNA by more binding modes, whose mutual distribution is dependent on the compound/ct-DNA ratio. The ‘‘acyclic’’ analogues **4**–**6** as well as cyclic’’ analogue **7** seem to interact mostly within the minor groove of DNA, although partial intercalation of **6** and **7** cannot be excluded. The ‘‘cyclic’’ analogues **8** and **9** at conditions of high excess of DNA over compounds concentration (best presented in fluorimetric titrations) most likely intercalate between DNA base pairs. However, for all studied compounds close to equimolar conditions in respect to DNA base pairs and in excess of compound over DNA, other binding modes are observed (decrease of UV–vis and fluorescence spectra, CD and LD spectroscopy, ΔT_m experiments), most probably as a result of agglomeration and stacking of the non-intercalated positively charged molecules along the negatively charged polynucleotide [44].

Here-presented results do not fit in our previously reported concept of photoinduced anticancer therapy [33] because there is no real difference in cytotoxicity against cell lines between the ‘‘acyclic’’ and ‘‘cyclic’’ derivatives and in addition the irradiation time necessary for photochemical dehydrocyclization is very long. Besides, it seems that, when isopropylamidino substituent [33] is attached directly to the naphthofuran

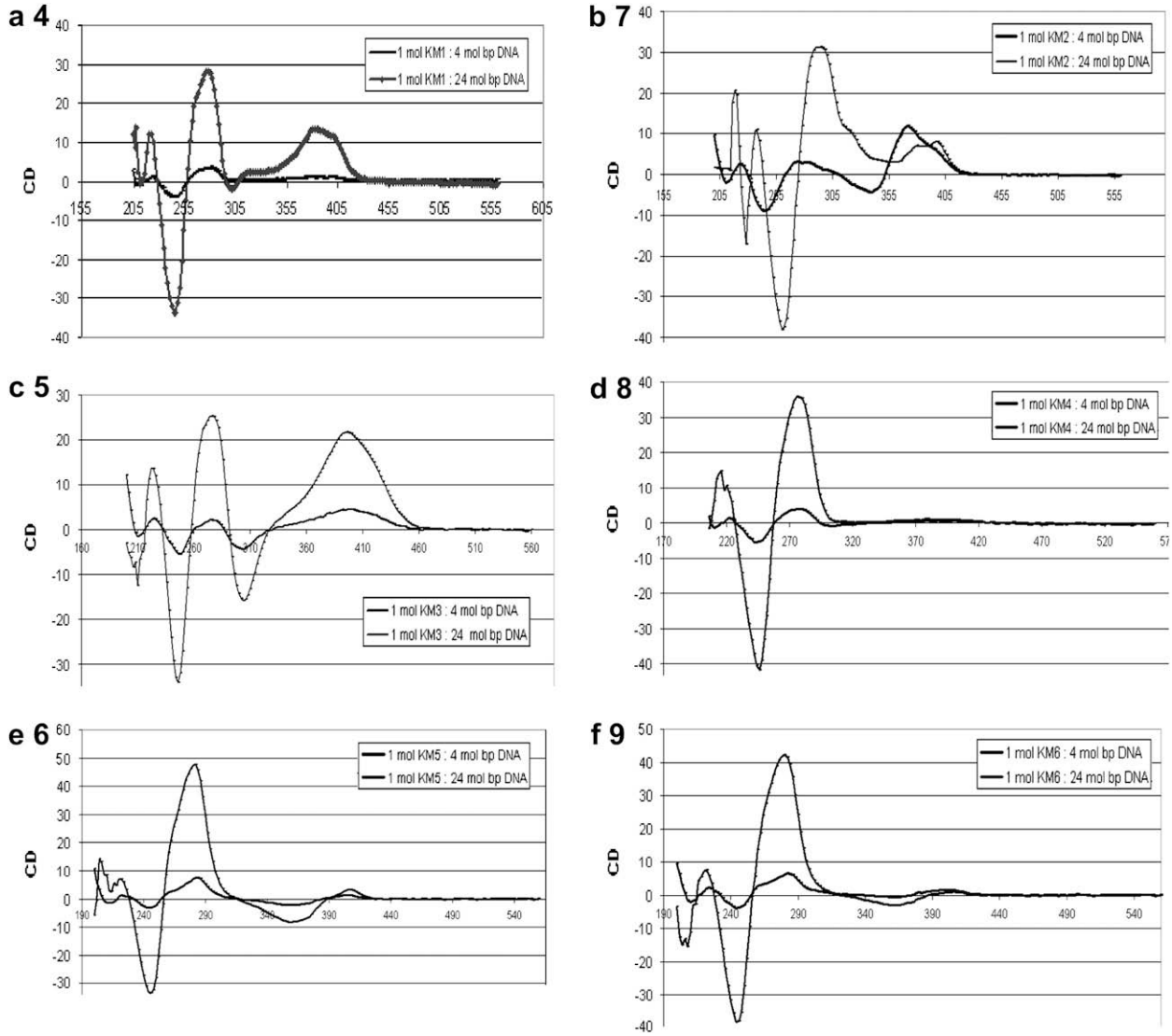

Fig. 9. CD spectra of compounds **4–9** in the presence of ct-DNA at two different mixing ratios, namely, dye/base pair, of 1:24 and 1:4.

moiety, the small planar molecule intercalates into the DNA, while large isopropylamidinobenzimidazolyl substituent of compounds **4–6** and **7–9** presented in this manuscript either hampers intercalation (**7**) or allows mixed binding modes aside DNA intercalation.

4. Experimental protocols

4.1. Chemistry

Melting points were recorded on an Original Kofler Mikroheitztisch apparatus (Reichert, Wien). The ^{1}H and ^{13}C NMR spectra were recorded on a Varian Gemini 300 or a Bruker Avance DPX 300 and 500 spectrometer at 300, 500 and 75 MHz, respectively. All NMR spectra were measured in DMSO-d_6 solutions using TMS as an internal standard. All compounds were routinely checked by TLC with Merck silica gel 60F-254 glass plates. Elemental analysis for carbon, hydrogen and nitrogen was performed on a Perkin–Elmer 2400 elemental analyzer. Where analyses are indicated only as symbols of elements, analytical results obtained are within 0.4% of the theoretical value.

*4.2. General method for preparation of compounds **4–6***

Solution of equimolar amounts of 4-*N*-isopropylamidino-1,2-phenylenediamine, corresponding aldehydes **1–3** and *p*-benzoquinone in absolute ethanol was refluxed for 4–5 h. After reaction mixture was cooled to room temperature, diethylether was added and the crude product was filtered off. The crude products were suspended in mixture of ethanol–acetone or water–acetone several times, until the powder products were analytically pure.

*4.2.1. Methyl-E-3-[5-(5-N-isopropylamidino-2-benzimidazolyl)-2-furyl]-2-phenyl-acrylate hydrochloride (**4**) [25]*

Compound **4** was prepared from **1** (1.01 g, 4.0 mmol), 4-*N*-isopropylamidino-1,2-phenylenediamine (0.90 g, 4.0 mmol) and *p*-benzoquinone (0.43 g, 4.0 mmol) in absolute EtOH (25 ml), after refluxing for 4 h, introduction of HCl gas into

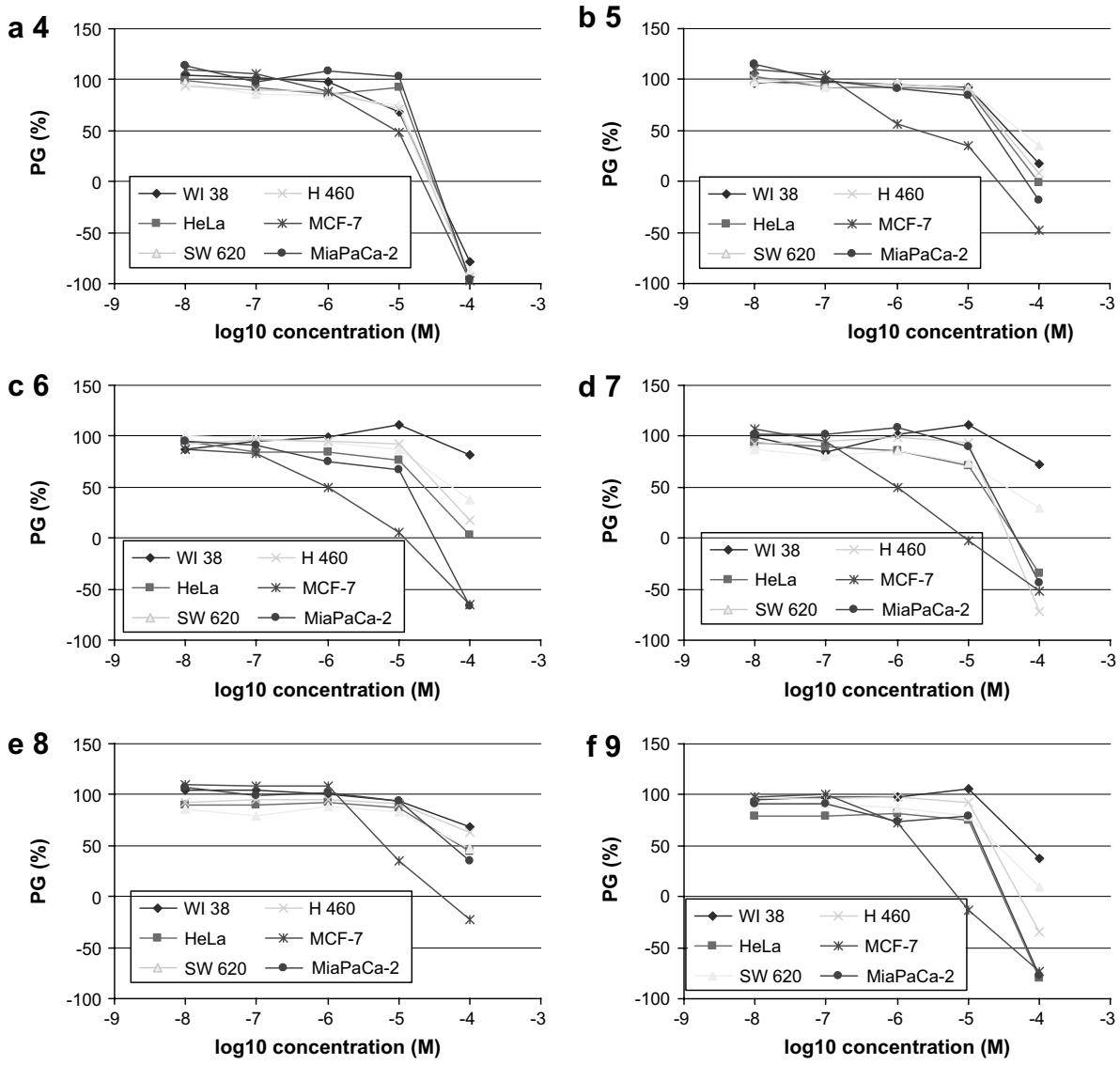

Fig. 10. Dose–response profiles for the compounds **4**–**9** tested on various human tumor cell lines in vitro. The cells were treated with the compounds at different concentrations, and percentage of growth (PG) was calculated. Each point represents a mean value of four parallel samples in three individual experiments.

suspension of crude product in absolute ethanol and precipitation from ethanol–acetone, in 0.95 g yield (41%) as slightly green powder; m.p. 234–236 °C (Ref. [25], m.p. 235–237 °C). ^{1}H NMR (δ/ppm) (300 MHz, DMSO-d_6): 13.54 (s, $NH_{\text{benzimidazole}}$, 1H), 9.60 (s, NH_{amidine}, 1H,), 9.57 (s, NH_{amidine}, 1H), 9.49 (br s, NH_{amidine}, 1H), 8.01 (s, 1H), 7.77 (d, $J = 8.7$ Hz, H_{arom}, 1H), 7.73 (s, 1H), 7.61 (d, $J = 8.8$ Hz, H_{arom}, 1H,), 7.54–7.46 (m, 3H), 7.38 (d, $J = 3.8$ Hz, H_{furyl}, 1H), 7.31 (d, $J = 7.8$ Hz, H_{arom}, 2H), 5.71 (d, $J = 3.8$ Hz, H_{furyl}, 1H), 4.07 (m, *CH*, 1H), 3.90 (s, OCH_3, 3H), 1.34 (d, $J = 6.2$ Hz, CH(CH_3)$_2$, 6H); ^{13}C NMR (δ/ppm) (300 MHz, DMSO-d_6): 166.9 (s), 162.5 (s), 152.9 (s), 145.6 (s), 144.4 (s), 135.5 (s), 134.45 (s), 132.9 (s), 129.6 (d, 2C), 129.3 (d), 129.1 (d, 2C), 127.1 (d), 124.7 (d), 124.2 (s), 119.87 (s), 116.8 (d), 116.6 (d), 116.2 (d), 115.3 (d), 53.1 (q), 45.7 (d), 21.9 (q, 2C). Elemental analysis calcd (%) for $C_{25}H_{27}N_4O_3Cl_3 \cdot 3H_2O$: C 50.71; H 5.62; N 9.43. Found: C 50.34; H 5.68; N 9.04.

Table 6
In vitro growth inhibition of various tumor cell lines

Compound	IC_{50}[a] (μM)					
	WI 38	HeLa	MiaPaCa-2	SW 620	MCF-7	H 460
4	13[b]	17 ± 0.2	19 ± 0.7	14 ± 0.9	9 ± 2	13 ± 0.1
5	36 ± 20	28 ± 13.5	21 ± 13	62 ± 32	2 ± 2	31 ± 0.1
6	>100	30 ± 28.6	13 ± 5	62 ± 36.9	1 ± 0.2	37 ± 1.6
7	>100	18 ± 12	21 ± 4.2	35 ± 23.8	1 ± 0.6	18 ± 0.2
8	>100	72 ± 29	61 ± 40	85 ± 10	6 ± 2	>100
9	71 ± 14	15 ± 0.5	16 ± 3	29 ± 15	2 ± 0.7	24 ± 8

[a] IC_{50} – the concentration that causes 50% growth inhibition.
[b] Only one experiment was performed.

*4.2.2. Ethyl-E-3-[5-(5-N-isopropylamidino-2-benzimidazolyl)-2-furyl]-2-(4-cyano)phenyl-acrylate hydrochloride (**5**)*

Compound **5** was prepared from **2** (0.20 g, 0.68 mmol), 4-*N*-isopropylamidino-1,2-phenylenediamine (0.090 g, 0.68 mmol) and *p*-benzoquinone (0.073 g, 0.68 mmol) in absolute EtOH

(10 ml), after refluxing for 5 h and recrystallization from ethanol–acetone, in 0.096 g yield (30%) as yellow powder; m.p. 210–212 °C. ^{1}H NMR (δ/ppm) (300 MHz, DMSO-d_6): 13.70 (s, $NH_{benzimidazole}$, 1H), 9.53 (s, $NH_{amidine}$, 1H), 9.40 (s, $NH_{amidine}$, 1H), 8.98 (br s, $NH_{amidine}$, 1H), 8.03 (s, 1H), 7.96 (d, $J = 7.86$ Hz, H_{arom}, 2H), 7.76 (s, 1H), 7.68 (d, 1H, $J = 8.70$ Hz, H_{arom}), 7.57 (d, $J = 8.60$ Hz, H_{arom}, 1H), 7.55 (d, $J = 7.65$ Hz, 2H), 7.32 (d, $J = 3.76$ Hz, H_{furyl}, 1H), 6.13 (d, $J = 3.76$ Hz, H_{furyl}, 1H), 4.21 (q, $J = 6.87$ Hz, OCH_2CH$_3$, 2H), 4.09–4.04 (m, *CH*, 1H), 1.29 (d, $J = 6.18$ Hz, CH(CH_3)$_2$, 6H), 1.23 (t, $J = 7.17$ Hz, OCH$_2$$CH_3$, 3H). Elemental analysis calcd (%) for $C_{27}H_{26}ClN_5O_3$: C 64.35; H 5.20; N 13.90. Found: C 64.41; H 5.12; N 13.87.

4.2.3. Methyl-E-3-[5-(5-N-isopropylamidino-2-benzimidazolyl)-2-thienyl]-2-phenyl-acrylate hydrochloride (6)

Compound **6** was prepared from **3** (0.60 g, 2.2 mmol), 4-*N*-isopropylamidino-1,2-phenylenediamine (0.50 g, 2.2 mmol) and *p*-benzoquinone (0.24 g, 2.2 mmol) in absolute EtOH (20 ml), after refluxing for 4 h and recrystallization from water–acetone, in 0.52 g yield (51%) as green powder; m.p. 229–231 °C. ^{1}H NMR (δ/ppm) (300 MHz, DMSO-d_6): 13.98 (br s, $NH_{benzimidazole}$, 1H), 9.49 (s, $NH_{amidine}$, 1H), 9.34 (s, $NH_{amidine}$, 1H), 8.99 (br s, $NH_{amidine}$, 1H), 8.08 (s, 1H), 7.99–7.92 (m, 2H), 7.70 (br s, 1H), 7.64 (d, $J = 4.05$ Hz, $H_{thienyl}$, 1H), 7.56–7.54 (m, 1H), 7.53 (d, $J = 7.80$ Hz, H_{arom}, 2H), 7.51 (d, $J = 3.20$ Hz, $H_{thienyl}$, 1H), 7.30–7.27 (m, 2H), 4.12–4.09 (m, *CH*, 1H), 3.30 (s, OCH_3, 3H), 2.05 (d, $J = 6.10$ Hz, CH(CH_3)$_2$, 6H); ^{13}C NMR (δ/ppm) (300 MHz, DMSO-d_6): 169.20 (s), 167.27 (s), 162.74 (s), 161.09 (s), 143.34 (s), 136.45 (s), 136.37 (d), 136.08 (s), 134.72 (s), 134.22 (s), 133.26 (d), 129.55 (s), 129.08 (d), 128.50 (d), 127.99 (d), 126.59 (d), 123.88 (d), 122.97 (d), 122.47 (s), 119.20 (d), 112.53 (d), 112.01 (d), 52.74 (q), 45.46 (d), 21.73 (q, 2C). Elemental analysis calcd (%) for $C_{25}H_{25}N_4O_2SCl$: C 62.42; H 5.24; N 11.65. Found: C 62.30; H 5.48; N 11.84; S 6.92.

4.3. General method for the preparation of compounds 7–9

Ethanolic solutions of compounds **4**–**6** and small amount of iodine (5%) were irradiated at room temperature, with 400-W high-pressure mercury lamp, using a Pyrex filter for about 20–80 h until the UV spectra show that the reaction of dehydrocyclization was finished. The air was bubbled through the solution. The solutions were concentrated under reduced pressure, diethylether was added and resulting products were filtered off and washed with diethylether. After precipitating from ethanol–diethylether or recrystallization from acetone–water, powder products were obtained.

4.3.1. Methyl 2-[(5-N-isopropylamidino)benzimidazolyl] naphtho[2,1-b]furan-5-carboxylate hydrochloride (7) [25]

Compound **7** was prepared from solution of **4** (0.90 g, 2.0 mmol) in ethanol (140 ml), after irradiation for 20 h and recrystallization from acetone–water, in 0.37 g yield (35%) as yellow powder; m.p. 256–258 °C (Ref. [25], m.p. 255–257 °C). ^{1}H NMR (δ/ppm) (300 MHz, DMSO-d_6): 13.65 (s, $NH_{benzimidazole}$, 1H), 9.62 (br s, $NH_{amidine}$, 1H), 9.52 (s, $NH_{amidine}$, 1H), 9.07 (s, $NH_{amidine}$, 1H), 8.88 (d, $J = 8.71$ Hz, H_{arom}, 1H), 8.63 (s, 1H), 8.50 (d, $J = 8.40$ Hz, H_{arom}, 1H), 8.47 (d, $J = 7.60$ Hz, H_{arom}, 1H), 8.11 (s, 1H), 7.87–7.70 (m, 3H), 7.63 (br s, 1H), 4.46 (m, *CH*, 1H), 4.07 (s, OCH_3, 3H), 1.24 (d, $J = 6.21$ Hz, CH(CH_3)$_2$, 6H); ^{13}C NMR (δ/ppm) (300 MHz, DMSO-d_6): 167.5 (s), 162.7 (s), 158.9 (s), 151.2 (s), 148.7 (s), 145.6 (s), 143.8 (s), 141.7 (s), 128.3 (d), 128.1 (s), 127.5 (d), 127.0 (d), 126.3 (d), 124.9 (s), 124.3 (d), 123.7 (d), 117.3 (s), 116.3 (d), 115.7 (d), 114.4 (d), 53.1 (q), 45.6 (d), 21.9 (q, 2C). Elemental analysis calcd (%) for $C_{25}H_{24}N_4O_3Cl_2 \cdot 2H_2O$: C 56.12; H 5.27; N 10.47. Found: C 56.30; H 5.16; N 10.72.

4.3.2. Ethyl 2-[(5-N-isopropylamidino)benzimidazolyl]-4-cyanonaphtho[2,1-b]furan-5-carboxylate hydrochloride (8)

Compound **8** was prepared from solution of **5** (0.07 g, 0.15 mmol) in ethanol (25 ml), after irradiation for 80 h and recrystallization from ethanol–diethylether, in 0.030 g yield (42%) as yellow powder; m.p. 229–231 °C. ^{1}H NMR (δ/ppm) (300 MHz, DMSO-d_6): 14.25 (s, $NH_{benzimidazole}$, 1H), 9.62 (br s, $NH_{amidine}$, 2H), 9.44 (s, $NH_{amidine}$, 1H), 9.22 (s, 1H), 9.05 (d, $J = 8.70$ Hz, H_{arom}, 1H), 9.03 (s, 1H), 8.64 (s, 2H), 7.99 (d, $J = 8.65$ Hz, H_{arom}, 1H), 7.79 (br s, 1H), 7.64 (d, $J = 8.00$ Hz, H_{arom}, 1H), 4.45 (q, $J = 7.00$ Hz, OCH_2CH$_3$, 2H), 4.05–4.02 (m, *CH*, 1H), 3.40 (s, OCH_3, 3H), 1.40 (t, $J = 6.90$ Hz, OCH$_2$$CH_3$, 3H), 1.26 (d, $J = 6.15$ Hz, CH(CH_3)$_2$, 6H); ^{13}C NMR (δ/ppm) (300 MHz, DMSO-d_6): 166.40 (s), 162.99 (s), 162.81 (s), 151.59 (s), 149.90 (s), 143.20 (s), 131.07 (d), 128.32 (s), 128.30 (s), 128.27 (d), 128.21 (d), 128.18 (d), 127.33 (s), 126.02 (s), 125.68 (s), 125.40 (d), 121.88 (d), 119.27 (s), 119.16 (d), 119.05 (d), 110.20 (s), 109.80 (d), 62.14 (t), 53.32 (q), 45.53 (d), 27.74 (d, 2C). Elemental analysis calcd (%) for $C_{26}H_{22}N_5O_3Cl$: C 64.00; H 4.54; N 14.35. Found: C 64.20; H 4.36; N 14.62.

4.3.3. Methyl 2-[(5-N-isopropylamidino)benzimidazolyl] naphtho[2,1-b]thiophen-5-carboxylate hydrochloride (9)

Compound **9** was prepared from solution of **6** (0.10 g, 0.21 mmol) in ethanol (30 ml), after irradiation for 40 h and precipitation from ethanol–diethylether, in 0.60 g yield (59%) as yellow powder; m.p. 247–249 °C. ^{1}H NMR (δ/ppm) (300 MHz, DMSO-d_6): 14.35 (s, $NH_{benzimidazole}$, 1H), 9.60 (br s, $NH_{amidine}$, 1H), 9.47 (s, $NH_{amidine}$, 1H), 9.32 (s, $NH_{amidine}$, 1H), 9.04 (s, 1H), 8.87 (d, $J = 8.28$ Hz, H_{arom}, 1H), 8.82 (s, 1H), 8.51 (d, $J = 8.20$ Hz, H_{arom}, 1H), 8.11 (d, $J = 7.60$ Hz, H_{arom}, 1H), 7.87–7.72 (m, 2H), 7.83 (s, 1H), 7.58 (br s, 1H), 4.12–4.08 (m, *CH*, 1H), 3.98 (s, OCH_3, 3H), 1.31 (d, $J = 6.10$ Hz, CH(CH_3)$_2$, 6H); ^{13}C NMR (δ/ppm) (300 MHz, DMSO-d_6): 167.01 (s), 162.34 (s), 162.32 (s), 154.36 (s), 147.82 (s), 139.12 (s), 136.53 (s), 136.35 (s), 133.56 (s), 129.09 (s), 128.04 (s), 127.59 (d), 127.55 (d), 126.31 (d), 125.34 (d), 124.95 (s), 123.96 (d), 121.62 (s), 119.80 (d), 118.65 (s), 117.63 (d), 115.38 (d), 52.40 (q), 45.02 (d), 21.28 (q, 2C). Elemental analysis calcd (%) for

$C_{25}H_{23}N_4O_2SCl$: C 62.69; H 4.84; N 11.70. Found: C 62.80; H 4.99; N 11.86.

4.4. Interactions with DNA

The electronic absorption spectra were recorded on Varian Cary 100 Bio spectrometer and fluorescence emission spectra were recorded on Varian Eclipse fluorimeter, in both cases using quartz cuvettes (1 cm). The calf thymus DNA (ct-DNA) was purchased from Aldrich, dissolved in the sodium cacodylate buffer, $I = 0.05$ mol dm^{-3}, pH = 7, additionally sonicated and filtered through a 0.45 μm filter, and the concentration of corresponding solution was determined spectroscopically as the concentration of phosphates [45]. The measurements were performed in the aqueous buffer solution (pH = 7.0; sodium cacodylate buffer, $I = 0.05$ mol dm^{-3}). Under the experimental conditions used the absorbance and fluorescence intensities of studied compounds were proportional to their concentrations. Obtained data were corrected for dilution. In fluorimetric titrations, excitation wavelengths of 365 (**4**), 370 (**5**), 374 (**6**), 360 (**7**), 368 (8) and 370 (**9**) nm were used to avoid inner filter effects caused by absorption of excitation light by added polynucleotide and changes of fluorescence emission were monitored at 400 nm. Spectroscopic titrations were performed by adding portions of polynucleotide solution into the solution of the studied compound. The stability constant (K_s) and [bound compound]/[polynucleotide phosphate] ratio (n) were calculated according to the Scatchard equation by non-linear least-square fitting [46], giving excellent correlation coefficients (>0.999) for obtained values of K_s and n. Thermal melting curves for ct-DNA and its complexes with studied compounds were determined as previously described by following the absorption change at 260 nm as a function of temperature. The heating rate was 1 °C/min. The absorbance of the ligand was subtracted from every curve, and the absorbance scale was normalized. Obtained T_m values are the midpoints of the transition curves, determined from the maximum of the first derivative or graphically by a tangent method. Given ΔT_m values were calculated subtracting T_m of the free nucleic acid from T_m of complex. Every ΔT_m value here reported was the average of at least two measurements, the error in ΔT_m is ±0.5 °C. The flow LD and CD spectra were recorded on a JASCO-720 spectropolarimeter.

4.5. Antitumor evaluation assays

The HeLa (cervical carcinoma), MiaPaCa-2 (pancreatic carcinoma), SW 620 (colon carcinoma), MCF-7 (breast carcinoma), H 460 (lung carcinoma), and WI 38 (normal fibroblasts) cells were cultured as monolayers and maintained in Dulbecco's modified Eagle medium (DMEM) supplemented with 10% fetal bovine serum (FBS), 2 mM L-glutamine, 100 U/ml penicillin and 100 μg/ml streptomycin in a humidified atmosphere with 5% CO_2 at 37 °C. The cell lines were inoculated onto a series of 96-well microtiter plates on day 0, at $1-3 \times 10^4$ cells/ml, depending on the doubling times of specific cell line. Test agents were then added in five 10-fold dilutions (10^{-8}–10^{-4} M) and incubated for a further 72 h. Working dilutions were freshly prepared on the day of testing. The solvent (DMSO) was also tested for eventual inhibitory activity by adjusting its concentration to be the same as in working concentrations. After 72 h of incubation the cell growth rate was evaluated by performing the MTT assay, which detects dehydrogenase activity in viable cells, as described previously [23,26].

Acknowledgments

This study was supported by grants 125-0982464-1356, 098-0982464-2514, 098-0982914-2918 by the Ministry of Science, Education and Sports of the Republic of Croatia.

References

[1] C. Bailly, Curr. Med. Chem. 7 (2007) 39–58.
[2] M. Demeunynck, C. Bailly, W.D. Wilson, DNA and RNA Binders. From Small Molecules to Drugs, Wiley-VCH, Weinheim, 2002.
[3] R.B. Silverman, The Organic Chemistry of Drug Design and Drug Action, second ed. Elsevier Academic Press, Burlington, San Diego, USA, London, UK, 2004.
[4] R. Langer, Science 293 (2001) 58–59.
[5] D. Lednicer, Strategies for Organic Drug Synthesis and Design, John Wiley & Sons, New York, 1998.
[6] A.R. Katritzky, D.O. Tymoshenko, D. Monteux, V. Vvedensky, G. Nikonov, C.B. Cooper, M. Deshpande, J. Org. Chem. 65 (2000) 8059–8062.
[7] V. Martínez, V. Burgos, J. Alvarez-Builla, G. Fernández, A. Domingo, R. Garcia-Nieto, F. Gago, I. Manzanares, C. Cuevas, J.J. Vaquero, J. Med. Chem. 47 (2004) 1136–1148.
[8] S. Demirayak, U. Abu Mohsen, A. Cagri Karaburun, Eur. J. Med. Chem. 37 (2002) 255–260.
[9] M. Boiani, M. Gonzalez, Mini Rev. Med. Chem. 5 (2005) 409–424.
[10] H. Göker, S. Özden, S. Yıldız, D.W. Boykin, Eur. J. Med. Chem. 40 (2005) 1062–1069.
[11] M.A. Ismail, R. Brun, T. Wenzler, F.A. Tanious, W.D. Wilson, D.W. Boykin, Bioorg. Med. Chem. 12 (2004) 5405–5413.
[12] H. Göker, C. Kus, D.W. Boykin, S. Yıldız, N. Altanlar, Bioorg. Med. Chem. 10 (2002) 2589–2596.
[13] K. Starčević, M. Kralj, K. Ester, I. Sabol, M. Grce, K. Pavelić, G. Karminski-Zamola, Bioorg. Med. Chem. 15 (2007) 4419–4426.
[14] T. Fonseca, B. Gigante, M.M. Marques, L.T. Gilchrist, E. De Clercq, Bioorg. Med. Chem. 12 (2004) 103–112.
[15] D. Shugar, Pharmacol. Ther. 82 (1999) 315–335.
[16] R.J. Snow, et al., Bioorg. Med. Chem. Lett. 17 (2007) 3660–3666.
[17] G. Lemaire, C. Delescluse, M. Pralavorio, N. Ledirac, P. Lesca, R. Rahmani, Life Sci. 74 (2004) 2265–2278.
[18] (a) P. Karlovsky, A.W. De Cock, Anal. Biochem. 194 (1991) 192–197;
(b) A. Abu-Daya, P.M. Brown, K.R. Fox, Nucleic Acid Res. 23 (1995) 3385–3392.
[19] S. Murata, J. Kusba, G. Piszczek, I. Gryczynski, J. Lakowicz, Biopolymers 57 (2000) 306–315.
[20] T.C. Jenkins, Curr. Med. Chem. 7 (2000) 99–115.
[21] M.P. Singh, T. Joseph, S. Kumar, Y. Bathini, J.W. Lown, Chem. Res. Toxicol. 5 (1992) 597–607.
[22] (a) T.A. Fairley, R.R. Tidwell, I. Donkor, N.A. Naiman, K.A. Ohemeng, R.J. Lombardy, J.A. Bentley, M. Cory, J. Med. Chem. 36 (1993) 1746–1753;
(b) S. Wang, J.E. Hall, F.A. Tanious, W.D. Wilson, D.A. Patrick, D.R. McCurdy, B.C. Bender, R.R. Tidwell, Eur. J. Med. Chem. 34 (1999) 215–224.

[23] I. Jarak, M. Kralj, L. Šuman, G. Pavlović, J. Dogan Koružnjak, I. Piantanida, M. Žinić, K. Pavelić, G. Karminski-Zamola, J. Med. Chem. 48 (2005) 2346–2360.
[24] W.D. Wilson, B. Nguyen, F.A. Tanious, A. Mathis, J.E. Hall, C.E. Stephens, D.W. Boykin, Curr. Med. Chem. Anticancer Agents 5 (2005) 389–408.
[25] M. Hranjec, M. Grdiša, K. Pavelić, D.W. Boykin, G. Karminski-Zamola, Il Farmaco 58 (2003) 1319–1324.
[26] (a) K. Starčević, M. Kralj, I. Piantanida, L. Šuman, K. Pavelić, G. Karminski-Zamola, Eur. J. Med. Chem. 41 (2006) 925–939;
(b) G. Karminski-Zamola, D. Palanović, K. Jakopčić, Croat. Chem. Acta 49 (1977) 521–525.
[27] G.V. Boyd, in: Saul Patai (Ed.), Recent Advances in the Synthesis of Amidines, The Chemistry of Amidines and Imidates, vol. 2, John Willey & Sons, New York, 1991, p. 339.
[28] M. Bajić, G. Karminski-Zamola, Croat. Chem. Acta 65 (1992) 835–846.
[29] J.K.F. Geirsson, A.J. Kvaran, Photochem. Phothobiol. A: Chem. 144 (2001) 175–177.
[30] K. Starčević, D.W. Boykin, G. Karminski-Zamola, Heterocycl. Commun. 8 (2002) 221–226.
[31] G. Karminski-Zamola, L. Fišer-Jakić, K. Jakopčić, Tetrahedron 38 (1982) 1329–1335.
[32] F.B. Mallory, C.W. Malory, Org. React. 30 (1984) 1–456.
[33] K. Starčević, G. Karminski-Zamola, I. Piantanida, M. Žinić, L. Šuman, M. Kralj, J. Am. Chem. Soc. 127 (2005) 1074–1075.
[34] H.J. Karlsson, M.H. Berquist, P. Lincoln, G. Westman, Bioorg. Med. Chem. 12 (2004) 2369–2384.
[35] M. Eriksson, B. Nordén, Methods Enzymol. 340 (2001) 68–98.
[36] A. Seaton, C. Higgins, J. Mann, A. Baron, C. Bailly, S. Neidle, H. Van den Berg, Eur. J. Cancer 39 (2003) 2548–2555.
[37] M.M. Ramla, M.A. Omar, A.-M.M. El-Khamry, H.I. El-Diwani, Bioorg. Med. Chem. 14 (2006) 7324–7332.
[38] T. Mukhopadhyay, J. Sasaki, R. Ramesh, J.A. Roth, Clin. Cancer Res. 8 (2002) 2963–2969.
[39] M. Iwanari, M. Nakajima, R. Kizu, K. Hayakawa, T. Yokoi, Arch. Toxicol. 76 (2002) 287–298.
[40] M.S. Chua, E. Kashiyama, T.D. Bradshaw, S.F. Stinson, E. Brantley, E. Sausville, M.F.G. Stevens, Cancer Res. 60 (2000) 5196–5203.
[41] O. Hankinson, Annu. Rev. Pharmacol. Toxicol. 35 (1995) 307–340.
[42] M. Backlund, L. Weidolf, M. Ingelman-Sundberg, Eur. J. Biochem. 261 (1999) 66–71.
[43] A. Monks, E. Harris, C. Hose, J. Connelly, E.A. Sausville, Mol. Pharmacol. 63 (2003) 766–772.
[44] (a) M.K. Pall, J.K. Ghosh, Spectrochim. Acta 51 (1995) 489–498;
(b) H.W. Zimmermann, Angew. Chem., Int. Ed. Engl. 25 (1986) 115.
[45] (a) J.B. Chaires, N. Dattagupta, D.M. Crothers, Biochemistry 21 (1982) 3933–3940;
(b) B.S. Palm, I. Piantanida, M. Žinić, H.J. Schneider, J. Chem. Soc., Perkin Trans. 2 (2000) 385–392.
[46] (a) G. Scatchard, Ann. N.Y. Acad. Sci. 51 (1949) 660–672;
(b) J.D. McGhee, P.H. von Hippel, J. Mol. Biol. 103 (1976) 679.